

# Absence of Pauling's residual entropy in thermally equilibrated $\text{Dy}_2\text{Ti}_2\text{O}_7$

D. Pomaranski<sup>1,2,3</sup>, L. R. Yaraskavitch<sup>1,2,3</sup>, S. Meng<sup>1,2,3</sup>, K. A. Ross<sup>4,5</sup>, H. M. L. Noad<sup>4,5</sup>,  
H. A. Dabkowska<sup>4,5</sup>, B. D. Gaulin<sup>4,5,6</sup> and J. B. Kycia<sup>1,2,3</sup>\*

**The discovery of the spin-ice phase in  $\text{Dy}_2\text{Ti}_2\text{O}_7$  numbers among the most significant findings in magnetic materials in over a decade<sup>1-3</sup>. Spin ice has since been associated with the manifestation of magnetic monopoles<sup>4,5</sup> and may even inform our understanding of emergent quantum electrodynamics<sup>6</sup>. The spin-ice model is based on an elegant analogy to Pauling's model of geometrical frustration in water ice, and predicts the same residual entropy, as confirmed by numerous measurements<sup>1,2,7-11</sup>. Here we present results for the specific heat of  $\text{Dy}_2\text{Ti}_2\text{O}_7$ , demonstrating why previous measurements were unable to correctly capture its low-temperature behaviour. By carefully tracking the flow of heat into and out of the material, we observe a non-vanishing specific heat that has not previously been detected. This behaviour is confirmed in two samples of  $\text{Dy}_2\text{Ti}_2\text{O}_7$ , in which cooling below 0.6 K reveals a deviation from Pauling's residual entropy, calling into question the true magnetic ground state of spin ice.**

Although the simple spin-ice model does account for most observed properties of the pyrochlore oxides  $\text{Dy}_2\text{Ti}_2\text{O}_7$  and  $\text{Ho}_2\text{Ti}_2\text{O}_7$ , unsolved puzzles remain. Simulations have demonstrated that long-range dipolar interactions should lift the degeneracy of the spin-ice manifold of states, and give rise to a unique, ordered ground state<sup>12</sup>. The Melko–den Hertog–Gingras (MDG) phase (Fig. 1) was the first theoretical prediction of an ordered state in spin ice; discovered through a numerical loop algorithm<sup>12,13</sup>. So far, however, experimental work has been unsuccessful in observing the MDG phase, concluding that the large energy barrier for fluctuations out of the ice-rules manifold does not allow ordering to occur<sup>2,8-11</sup>.

Recent low-temperature measurements have determined that the spin relaxation time markedly increases as temperature is lowered. For example, magnetization<sup>14,15</sup> and a.c.-susceptibility<sup>16</sup> measurements show that the spin relaxation time in  $\text{Dy}_2\text{Ti}_2\text{O}_7$  is greater than  $10^4$  s below 0.45 K. Ref. 16 also reported Arrhenius behaviour with a barrier to relaxation of 9.79 K, much larger than the cost of a single spin flip of  $4J_{\text{eff}} = 4.44$  K, where  $J_{\text{eff}}$  is the nearest-neighbour effective exchange energy<sup>17</sup>. This difference could be due to monopole effects<sup>15</sup>, or many-body phenomena such as screening, but remains as a major open question<sup>18-21</sup>. Consequently, we would expect that thermal relaxation is dominated by this slow magnetic system in the spin-ice regime. These spin dynamics motivated us to re-measure the specific heat in a way that allows for extremely slow thermal equilibration.

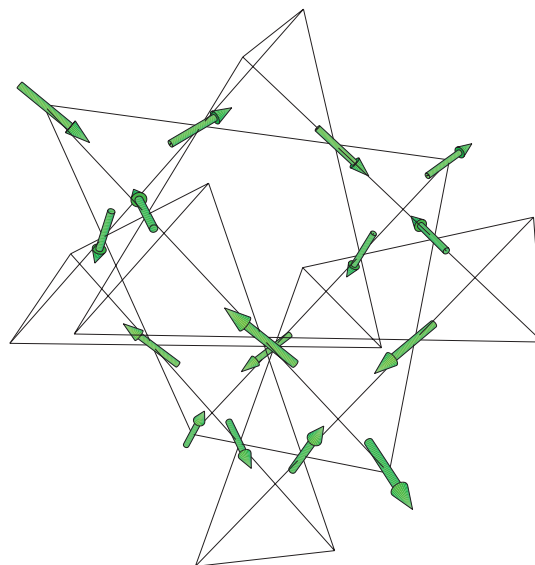


**Figure 1 | The pyrochlore lattice, with Dy spins at the vertices of corner-sharing tetrahedra. The MDG phase ( $\mathbf{q} = (0, 0, 2\pi/a)$  state), shown here, is a potential candidate for the long-range ordered state of  $\text{Dy}_2\text{Ti}_2\text{O}_7$  (ref. 12).**

All of our measurements were performed on a magnetically shielded dilution refrigerator at the University of Waterloo. Two samples of  $\text{Dy}_2\text{Ti}_2\text{O}_7$  were prepared at McMaster University using a procedure similar to that described in ref. 22. The needle-shaped single crystal was approximately  $2 \times 1 \times 1$  mm, and had a mass of 16.64 mg, and belongs to the same mother crystal studied in refs 15, 16. The second sample was prepared from sintered powder used in the growth of this crystal, which was mixed in a  $\sim 1:1$  volumetric ratio with  $3 \mu\text{m}$  silver powder to improve thermal conductivity. This mixture was then cold-pressed into a  $\sim 3$ -mm-diameter and  $\sim 2$ -mm-length cylinder composed of 49.28 mg  $\text{Dy}_2\text{Ti}_2\text{O}_7$ .

The details of the stoichiometry and chemical order in rare-earth titanate pyrochlores are of topical interest. In particular, stuffing wherein extra rare-earth ions occupy the Ti sublattice sites, has been shown to be a relevant form of disorder in single crystals of nominally stoichiometric  $\text{Yb}_{2+x}\text{Ti}_{2-x}\text{O}_{7-x/2}$  grown using the optical floating zone technique. Neutron diffraction has shown nominally

<sup>1</sup>Department of Physics and Astronomy, University of Waterloo, 200 University Avenue West, Waterloo, Ontario, N2L 3G1, Canada, <sup>2</sup>Guelph-Waterloo Physics Institute, University of Waterloo, 200 University Avenue West, Waterloo, Ontario, N2L 3G1, Canada, <sup>3</sup>Institute for Quantum Computing, University of Waterloo, 200 University Avenue West, Waterloo, Ontario, N2L 3G1, Canada, <sup>4</sup>Department of Physics and Astronomy, McMaster University, 1280 Main Street West, Hamilton, Ontario, L8S 4M1, Canada, <sup>5</sup>Brockhouse Institute for Materials Research, McMaster University, 1280 Main Street West, Hamilton, Ontario, L8S 4M1, Canada, <sup>6</sup>Canadian Institute for Advanced Research, 180 Dundas Street West, Toronto, Ontario, M5G1Z8, Canada.

\*e-mail: jkycia@uwaterloo.ca

stoichiometric ( $x = 0$ ) single-crystal samples to be weakly stuffed, with  $x = 0.046$  (2.3%) of the  $\text{Ti}^{4+}$  sublattice replaced with extra  $\text{Yb}^{3+}$  ions<sup>23</sup>. A sample variation in the low-temperature specific heat of  $\text{Yb}_2\text{Ti}_2\text{O}_7$  samples has been observed, which probably correlates with the presence and degree of the stuffing. The stoichiometry of  $\text{Dy}_2\text{Ti}_2\text{O}_7$  samples is anticipated to be more robust against the tendency for weak stuffing, as  $\text{Dy}^{3+}$  is a worse fit into the  $\text{Ti}^{4+}$  position compared with  $\text{Yb}^{3+}$  owing to its larger ionic radius<sup>24</sup>. Stuffing may also arise from evaporation of titanium oxide in the molten zone of the optical furnace. This would be less of an issue for the powder sample, which is prepared at lower temperatures. Magnetization measurements in ref. 15 estimated that the level of stuffing in our single crystal is 0.3% ( $x = 0.021$ ). The degree of stuffing for the powder sample should be less than or equal to the crystal.

We measured thermal relaxation to calculate the specific heat of  $\text{Dy}_2\text{Ti}_2\text{O}_7$ , using a sample configuration similar to that described in ref. 25. Our sample was connected to a thermal reservoir through a weak link of  $\text{Pt}_{91}\text{W}_9$  with conductance  $K/T \approx 2.8 \times 10^{-8} \text{ J K}^{-2} \text{ s}^{-1}$  and  $1.2 \times 10^{-7} \text{ J K}^{-2} \text{ s}^{-1}$  for the crystal and powder, respectively. By applying constant heat, the sample temperature was raised by  $\Delta T \sim 5\%$  to  $10\%$  above the thermal reservoir. The heat was then turned off, and temperature was recorded as it equilibrated back to the thermal reservoir. As energy is released from the sample, a temperature gradient,  $\Delta T(t)$ , develops across the weak link. This link is chosen to have a poor thermal conductance, to produce a measurable  $\Delta T(t)$  for very low levels of heat flow. The heat flow across this gradient is the product of  $\Delta T(t)$  and  $K$ . By integrating over time for the entire relaxation curve, we obtain the total energy released from the sample, which is directly related to the specific heat<sup>26</sup>.

Our typical relaxation curves are plotted in Fig. 2, normalized with respect to the total change in  $\Delta T$  (that is,  $\Delta T(t=0) - \Delta T(t \rightarrow \infty)$ ). Viewing the initial 1,000 s of data (Fig. 2a), it is clear that the integral of  $\Delta T(t)$  decreases with temperature. As specific heat,  $c(T)$ , is proportional to this integral, one might then conclude that  $c(T)$  is also vanishing with temperature. Extending the time axis beyond  $10^4$  s as done in Fig. 2b, it becomes evident that the specific heat is not decreasing with temperature below  $\sim 0.6$  K, but that the thermal relaxation is dominated by very slow processes. These processes impede the flow of heat into and out of the sample, requiring  $>100$  h for equilibrium below the lowest temperature measured (0.34 K). Without measuring for sufficient times, the total heat released by the sample for a given temperature change will be significantly underestimated. Consequently, this will result in an underestimation of the total specific heat. Previous specific-heat measurements were performed using either the quasi-adiabatic heat pulse method with an equilibration time window of 15 s, (ref. 2) or the thermal relaxation method with  $\sim 600$  s of relaxation<sup>27</sup>. Other reports did not specify their measurement times<sup>9–11</sup>. From our work in Fig. 2, it is evident that much longer equilibration times are necessary below 0.5 K.

The tail of each relaxation curve was fitted to an exponential function, which provides an estimate of the internal relaxation time constant. Such a fit is justifiable within a thermal decoupling model that is mathematically analogous to the internal  $\tau_2$  effect of relaxation calorimetry<sup>28</sup>. This effect becomes prominent in our crystal of  $\text{Dy}_2\text{Ti}_2\text{O}_7$  below  $\sim 0.6$  K where a number of factors may be responsible, such as thermal decoupling of magnetic and phonon contributions. As shown in Fig. 2b (inset), our single-crystal relaxation time constants show close agreement with the Arrhenius behaviour determined from a.c.-susceptibility<sup>16</sup> and magnetization<sup>14,15</sup> measurements (Fig. 2b inset).

The resulting specific heat in Fig. 3 shows excellent agreement with the literature above 0.6 K (refs 8–11). Below this temperature, we observed a feature that has not been measured in previous experiments. By limiting our analysis to the first 600 s of thermal relaxation, we can qualitatively reproduce the results of previous

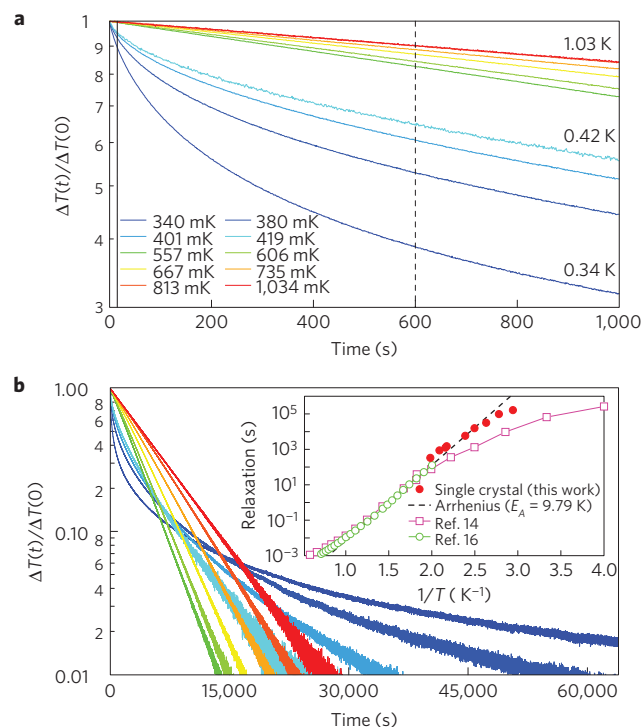


**Figure 2 | Normalized thermal relaxation,  $\Delta T(t)/\Delta T(0)$  versus time, at various nominal temperatures,  $T$ , for single-crystal  $\text{Dy}_2\text{Ti}_2\text{O}_7$ .**

**a**, Relaxation data shown up to 1,000 s. Other works acquired the thermal relaxation only for  $\leq 600$  s (dashed vertical line)<sup>27</sup>. Similarly, results employing the quasi-adiabatic heat pulse method were limited to an equilibration time window of  $\sim 15$  s (dotted vertical line)<sup>2</sup>. Typical  $\Delta T$  are  $\sim 5$ – $10\%$  of the nominal temperature,  $T$ . **b**, The same relaxation curves as in **a**, with the time axis extended beyond 1,000 s. Inset, the long internal time constants measured below 0.5 K agree with the Arrhenius behaviour observed by magnetic measurements above 0.5 K (refs 14,16).

experiments (Fig. 3). This provides compelling evidence that magnetic ordering in  $\text{Dy}_2\text{Ti}_2\text{O}_7$  must indeed occur on very long timescales<sup>12</sup>. The total entropy,  $s(T)$ , was computed by integrating  $c(T)/T$  from 0.34 to 1 K, and using data from ref. 8 above 1 K (Fig. 4). Whereas previous measurements found a finite residual entropy equivalent to Pauling's entropy for water ice ( $(R/2)\ln(3/2)$ ), our measurements reveal no evidence of a plateau at this value. We considered the possibility of a spin-glass transition at lower temperatures, but our data would not fit a Schottky curve without having negative entropy at zero temperature.

In the classical spin-ice model, entropy due to monopoles (that is, 3-in 1-out and 1-in 3-out tetrahedral spin states) and higher excitations (that is, 4-in or 4-out spin states) should be removed at low temperatures. The remaining entropy represents the disorder of a highly degenerate 2-in-2-out state for each tetrahedron, which is equal to Pauling's value  $(R/2)\ln(3/2)$ . Our work suggests that this characteristic of spin ice does not hold for a thermally equilibrated sample. The fact that previous, short-timescale ( $\leq 600$  s) measurements<sup>2,8–11</sup> obtain Pauling's residual entropy shows that ordering of the 2-in-2-out states must also occur in this time period. Owing to this feature in the material's intrinsic timescales and its ability to quench, certain experiments are able to observe spin-ice characteristics at temperatures below 0.6 K. The true ground state is observed only on much longer timescales.

Our experiment was designed to be capable of observing the slow magnetic relaxation that arises below  $\sim 0.6$  K. We observed a marked increase in the thermal relaxation time of single-crystal  $\text{Dy}_2\text{Ti}_2\text{O}_7$  (Fig. 2b inset) from  $\sim 10^3$  s at 0.45 K,

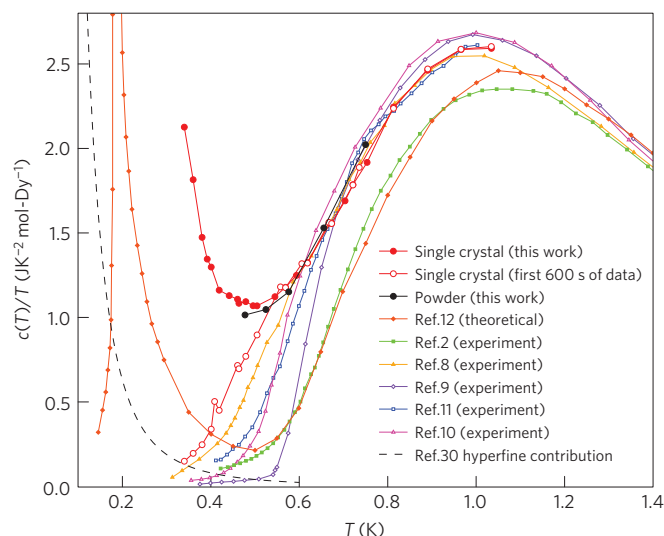


**Figure 3 | Specific heat versus temperature of  $\text{Dy}_2\text{Ti}_2\text{O}_7$  in zero field.** Previous experimental results had no signature of an upturn below 0.6 K (refs 2,8–11). The Dy nuclear hyperfine contribution (dashed line) is insignificant at these temperatures<sup>30</sup>.

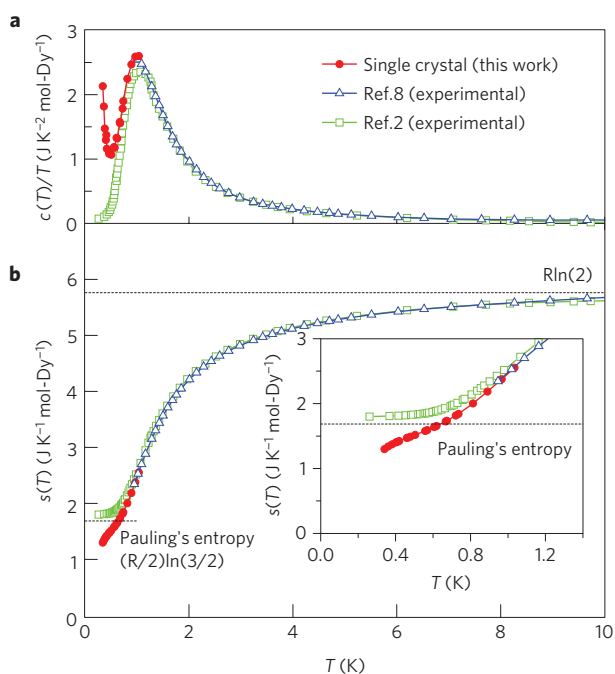


**Figure 4 | Specific heat and entropy for single-crystal  $\text{Dy}_2\text{Ti}_2\text{O}_7$  versus temperature.** **a**, Specific heat divided by temperature,  $c(T)/T$ , was integrated from 0.34 to 12 K, where data from ref. 8 were used above 1 K. **b**, The resulting cumulative entropy does not plateau at Pauling's residual value, as was previously reported<sup>2</sup>. Inset shows low-temperature detail.

to approximately  $10^5$  s at 0.34 K. These timescales are also consistent with the Arrhenius behaviour observed with magnetic measurements<sup>14–16</sup>, which provides compelling evidence that spin relaxation is responsible for the slow thermal relaxation. Our measurements became restricted by long timescales below 0.34 K (0.45 K for the powder sample), where the material can require > 1 week of equilibration. These timescales should provide guidance for any experiment (for example,  $\mu\text{SR}$  or neutron scattering) aimed at probing equilibrium characteristics of  $\text{Dy}_2\text{Ti}_2\text{O}_7$  in this temperature range.

We have shown, contrary to popular understanding from the body of experimental work so far, that thermally equilibrated, nominally stoichiometric  $\text{Dy}_2\text{Ti}_2\text{O}_7$  does not possess Pauling's entropy at zero temperature (Fig. 4). Furthermore, the absence of a low-temperature plateau in the entropy at Pauling's value provides powerful evidence that the spin-ice state in  $\text{Dy}_2\text{Ti}_2\text{O}_7$  disappears once the long internal equilibration times of this material are accounted for. By measuring over short timescales, earlier investigations that obtain Pauling's residual entropy were able to capture spin-ice-like properties even at the lowest temperatures. We conclude that the ground state of thermally equilibrated  $\text{Dy}_2\text{Ti}_2\text{O}_7$  is not a degenerate manifold of spin-ice states, and therefore its effect on spin-ice and monopole characteristics calls for further study.

The question still remains: what is the true ground state of spin ice? Although the MDG model does agree qualitatively with our results, it may be improved by the inclusion of perturbative spin exchanges beyond the nearest neighbour<sup>29</sup>. The mechanisms responsible for spin dynamics leading up to an ordered state may be attributable to cluster-like processes involving six or more spins, instead of the less energetically favourable single-monopole event<sup>12,13</sup>. Compelling evidence for this type of process has already been suggested by quantum mechanical models of spin ice, where the Pauling degeneracy is lifted by a ground state formed through the coherent superposition of classical spin-ice configurations<sup>6</sup>.

Received 12 June 2012; accepted 22 February 2013;  
published online 7 April 2013

## References

- Harris, M. J., Bramwell, S. T., McMorro, D. F., Zeiske, T. & Godfrey, K. W. Geometrical frustration in the ferromagnetic pyrochlore  $\text{Ho}_2\text{Ti}_2\text{O}_7$ . *Phys. Rev. Lett.* **79**, 2554–2557 (1997).
- Ramirez, A. P., Hayashi, A., Cava, R. J., Siddharthan, R. & Shastry, B. S. Zero-point entropy in spin ice. *Nature* **399**, 333–335 (1999).
- Bramwell, S. T. & Gingras, M. J. P. Spin ice state in frustrated magnetic pyrochlore materials. *Science* **294**, 1495–1501 (2001).
- Ryzhkin, I. Magnetic relaxation in rare-earth oxide pyrochlores. *J. Exp. Theor. Phys.* **101**, 481–486 (2005).
- Castelnovo, C., Moessner, R. & Sondhi, S. L. Magnetic monopoles in spin ice. *Nature* **451**, 42–45 (2008).
- Shannon, N., Sikora, O., Pollmann, F., Penc, K. & Fulde, P. Quantum ice: A quantum Monte Carlo study. *Phys. Rev. Lett.* **108**, 067204 (2012).
- Pauling, L. The structure and entropy of ice and of other crystals with some randomness of atomic arrangement. *J. Am. Chem. Soc.* **57**, 2680–2684 (1935).
- Klemke, B. *et al.* Thermal relaxation and heat transport in the spin ice material  $\text{Dy}_2\text{Ti}_2\text{O}_7$ . *J. Low Temp. Phys.* **163**, 345–369 (2011).
- Higashinaka, R., Fukazawa, H., Yanagishima, D. & Maeno, Y. Specific heat of  $\text{Dy}_2\text{Ti}_2\text{O}_7$  in magnetic fields: Comparison between single-crystalline and polycrystalline data. *J. Phys. Chem. Solids* **63**, 1043–1046 (2002).
- Morris, D. J. P. *et al.* Dirac strings and magnetic monopoles in the spin ice  $\text{Dy}_2\text{Ti}_2\text{O}_7$ . *Science* **326**, 411–414 (2009).
- Kadowaki, H. *et al.* Observation of magnetic monopoles in spin ice. *J. Phys. Soc. Jpn* **78**, 103706 (2009).
- Melko, R. G., den Hertog, B. C. & Gingras, M. J. P. Long-range order at low temperatures in dipolar spin ice. *Phys. Rev. Lett.* **87**, 067203 (2001).
- Melko, R. G. & Gingras, M. J. P. Monte Carlo studies of the dipolar spin ice model. *J. Phys. Condens. Matter* **16**, R1277 (2004).
- Matsuhira, K. *et al.* Spin dynamics at very low temperature in spin ice  $\text{Dy}_2\text{Ti}_2\text{O}_7$ . *J. Phys. Soc. Jpn* **80**, 123711 (2011).
- Revell, H. M. *et al.* Evidence of impurity and boundary effects on magnetic monopole dynamics in spin ice. *Nature Phys.* **9**, 34–37 (2012).
- Yaraskavitch, L. R. *et al.* Spin dynamics in the frozen state of the dipolar spin ice material  $\text{Dy}_2\text{Ti}_2\text{O}_7$ . *Phys. Rev. B* **85**, 020410 (2012).
- Gardner, J. S., Gingras, M. J. P. & Greedan, J. E. Magnetic pyrochlore oxides. *Rev. Mod. Phys.* **82**, 53–107 (2010).
- Jaubert, L. D. C. & Holdsworth, P. C. W. Signature of magnetic monopole and Dirac string dynamics in spin ice. *Nature Phys.* **5**, 258–261 (2009).
- Bramwell, S. T. *et al.* Measurement of the charge and current of magnetic monopoles in spin ice. *Nature* **461**, 956–959 (2009).
- Jaubert, L. D. C. & Holdsworth, P. C. W. Magnetic monopole dynamics in spin ice. *J. Phys. Condens. Matter* **23**, 164222 (2011).
- Giblin, S. R., Bramwell, S. T., Holdsworth, P. C. W., Prabhakaran, D. & Terry, I. Creation and measurement of long-lived magnetic monopole currents in spin ice. *Nature Phys.* **7**, 252–258 (2011).

22. Gardner, J. S., Gaulin, B. D. & Paul, D. McK. Single crystal growth by the floating-zone method of a geometrically frustrated pyrochlore antiferromagnet,  $\text{Tb}_2\text{Ti}_2\text{O}_7$ . *J. Cryst. Growth* **191**, 740–745 (1998).
23. Ross, K. A. *et al.* Lightly stuffed pyrochlore structure of single-crystalline  $\text{Yb}_2\text{Ti}_2\text{O}_7$  grown by the optical floating zone technique. *Phys. Rev. B* **86**, 174424 (2012).
24. Shannon, R. D. Revised effective ionic radii and systematic studies of interatomic distances in halides and chalcogenides. *Acta Crystallogr. A* **32**, 751–767 (1976).
25. Quilliam, J. A., Mugford, C. G. A., Gomez, A., Kycia, S. W. & Kycia, J. B. Specific heat of the dilute Ising magnet  $\text{LiHo}_x\text{Y}_{1-x}\text{F}_4$ . *Phys. Rev. Lett.* **98**, 037203 (2007).
26. Tsujii, H., Andracka, B., Muttalib, K. A. & Takano, Y. Distributed  $\tau_2$  effect in relaxation calorimetry. *Physica B* **329–333**, 1552–1553 (2003).
27. Klemke, B. *Thermal Properties of Dysprosium-Titanate in the Spin Ice State* PhD thesis, Technische Universität Berlin (2010).
28. Shepherd, J. P. Analysis of the lumped  $\tau_2$  effect in relaxation calorimetry. *Rev. Sci. Instrum.* **56**, 273–277 (1985).
29. Yavors'kii, T., Fennell, T., Gingras, M. J. P. & Bramwell, S. T.  $\text{Dy}_2\text{Ti}_2\text{O}_7$  Spin ice: A test case for emergent clusters in a frustrated magnet. *Phys. Rev. Lett.* **101**, 037204 (2008).
30. Filippi, J., Lasjaunias, J. C., Ravex, A., Tchéou, F. & Rossat-Mignod, J. Specific heat of dysprosium gallium garnet between 37 mK and 2 K. *Solid State Commun.* **23**, 613–616 (1977).

### Acknowledgements

We thank R. G. Melko, H. M. Revell, M. J. P. Gingras, R. W. Hill, P. Henelius, C. L. Henley and A. D. Bianchi for helpful discussions. This research was financially supported by NSERC, CFI and OFI.

### Author contributions

K.A.R., H.M.L.N., H.A.D. and B.D.G. prepared the crystal and powder samples. D.P., L.R.Y., S.M. and J.B.K. designed and performed the specific-heat measurements. The manuscript was written by D.P. and J.B.K. with input and discussion from all authors.

### Additional information

Reprints and permissions information is available online at [www.nature.com/reprints](http://www.nature.com/reprints). Correspondence and requests for materials should be addressed to J.B.K.

### Competing financial interests

The authors declare no competing financial interests.